Leon, R. “Composite Connections”
Structural Engineering Handbook
Ed. Chen Wai-Fah
Boca Raton: CRC Press LLC, 1999

Composite Connections

Roberto Leon
School of Civil and Environmental Engineering, Georgia Institute of Technology, Atlanta, GA

23.1 Introduction

The vast majority of steel buildings built today incorporate a floor system consisting of composite beams, composite joists or trusses, stub girders, or some combination thereof [29]. Traditionally the strength and stiffness of the floor slabs have only been used for the design of simply-supported flexural members under gravity loads, i.e., for members bent in single curvature about the strong axis of the section. In this case the members are assumed to be pin-ended, the cross-section is assumed to be prismatic, and the effective width of the slab is approximated by simple rules. These assumptions allow for a member-by-member design procedure and considerably simplify the checks needed for strength and serviceability limit states. Although most structural engineers recognize that there is some degree of continuity in the floor system because of the presence of reinforcement to control crack widths over column lines, this effect is considered difficult to quantify and thus ignored in design.

The effect of the floor slabs has also been neglected when assessing the strength and stiffness of frames subjected to lateral loads for four principal reasons. First, it has been assumed that neglecting the additional strength and stiffness provided by the floor slabs always results in a conservative design. Second, a sound methodology for determining the M-θ curves for these connections is a prerequisite if their effect is going to be incorporated into the analysis. However, there is scant data available in order to formulate reliable moment-rotation (M-θ) curves for composite connections, which fall typically into the partially restrained (PR) and partial strength (PS) category. Third, it is difficult to incorporate into the analysis the non-prismatic composite cross-section that results when the member is subjected to double curvature as would occur under lateral loads. Finally, the degree of composite interaction in floor members that are part of lateral-load resisting systems in seismic areas is low, with most having only enough shear transfer capacity to satisfy diaphragm action.

Research during the past 10 years [25] and damage to steel frames during recent earthquakes [22] have pointed out, however, that there is a need to reevaluate the effect of composite action in modern frames. The latter are characterized by the use of few bents to resist lateral loads, with the ratio of number of gravity to moment-resisting columns often as high as 6 or more. In these cases the aggregate effect of many PR/PS connections can often add up to a significant portion of the lateral resistance of a frame. For example, many connections that were considered as pins in the analysis (i.e., connections to columns in the gravity load system) provided considerable lateral strength and stiffness to steel moment-resisting frames (MRFs) damaged during the Northridge earthquake. In these cases many of the fully restrained (FR) welded connections failed early in the load history, but the frames generally performed well. It has been speculated that the reason for the satisfactory performance was that the numerous PR/PS connections in the gravity load system were able to provide the required resistance since the input base shear decreased as the structure softened. In these PR/PS connections, much of the additional capacity arises from the presence of the floor slab which provides a moment transfer mechanism not accounted for in design.

In this chapter general design considerations for a particular type of composite PR/PS connection will be given and illustrated with examples for connections in braced and unbraced frames. Information on design of other types of bolted and composite PR connections is given elsewhere [22], (Chapter 6 of [29]). The chapter begins with discussions of both the development of M-θ curves and the effect of PR connections on frame analysis and design. A clear understanding of these two topics is essential to the implementation of the design provisions that have been proposed for this type of construction [26] and which will be illustrated herein.

23.2 Connection Behavior Classification

The first step in the design of a building frame, after the general topology, the external loads, the materials, and preliminary sizes have been selected, is to carry out an analysis to determine member forces and displacements. The results of this analysis depend strongly on the assumptions made in constructing the structural model. Until recently most computer programs available to practicing engineers provided only two choices (rigid or pinned) for defining the connections stiffness. In reality connections are very complex structural elements and their behavior is best characterized by M-θ curves such as those given in Figure 23.1 for typical steel connections to an A36 W24x55 beam ($M_{p,\text{beam}} = 4824$ kip-in.). In Figure 23.1, M_{conn} corresponds to the moment at the column face, while θ_{conn} corresponds to the total rotation of the connection and a portion of the beam generally taken as equal to the beam depth. These curves are shown for illustrative purposes only, so that the different connection types can be contrasted. For each of the connection types shown, the curves can be shifted through a wide range by changing the connection details, i.e., the thickness of the angles in the top and seat angle case.

While the M-θ curves are highly non-linear, at least three key properties for design can be obtained from such data. Figure 23.2 illustrates the following properties, as well as other relevant connection characteristics, for a composite connection:

1. Initial stiffness (k_{ser}), which will be used in calculating deflection and vibration performance under service loads. In these analysis the connection will be represented by a linear rotational spring. Since the curves are non-linear from the beginning, and k_{ser} will be assumed constant, the latter needs to be defined as the secant stiffness to some predetermined rotation.
2. Ultimate strength ($M_{u,\text{conn}}$), which will be used in assessing the ultimate strength of the frame. The strength is controlled either by the strength of the connection itself or that of the framing beam. In the former case the connection is defined as partial strength (PS) and in the latter as full strength (FS).
3. Maximum available rotation (θ_u), which will be used in checking both the redistribution capacity under factored gravity loads and the drift under earthquake loads. The

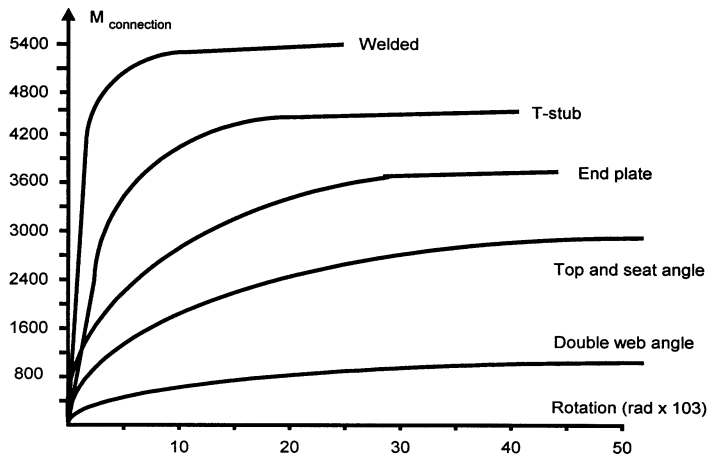

FIGURE 23.1: Typical moment-rotation curves for steel connections.

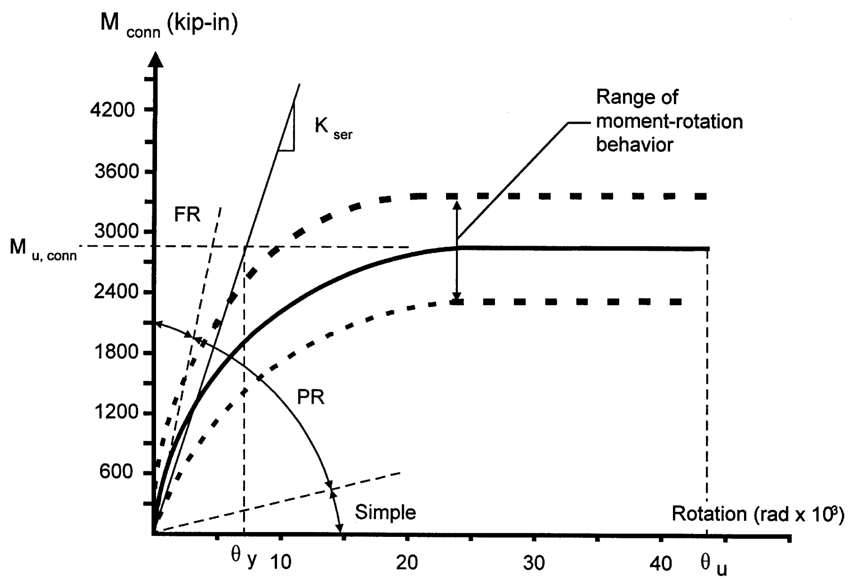

FIGURE 23.2: Definition of connection properties for PR connections.

required rotational capacity depends on the design assumptions and the redundancy of the structure.

It is often useful also to define a fourth quantity, the ductility (μ) of the connection. This is defined as the ratio of the ultimate rotation capacity (θ_u) to some nominal "yield" rotation (θ_y). It should be understood that the definition of θ_y is subjective and needs to account for the shape of the curve (i.e., how sharp is the transition from the service to the yield level — the sharper the transition the more valid the definition shown in Figure 23.2). In the design procedure to be discussed in this chapter, the initial stiffness, ultimate strength, maximum rotation, and ductility are properties that will need to be check by the structural engineer.

Figure 23.2 schematically shows that there can be a considerable range of strength and stiffness for these connections. The range depends on the specific details of the connection, as well as the normal variability expected in materials and construction practices. Figure 23.2 also shows that certain ranges of initial stiffness can be used to categorize the initial connection stiffness as either fully restrained (FR), partially restrained (PR), or simple. Because the connection behavior is strongly influenced by the strength and stiffness of the framing members, it is best to non-dimensionalize M-θ curves as shown in Figure 23.3.

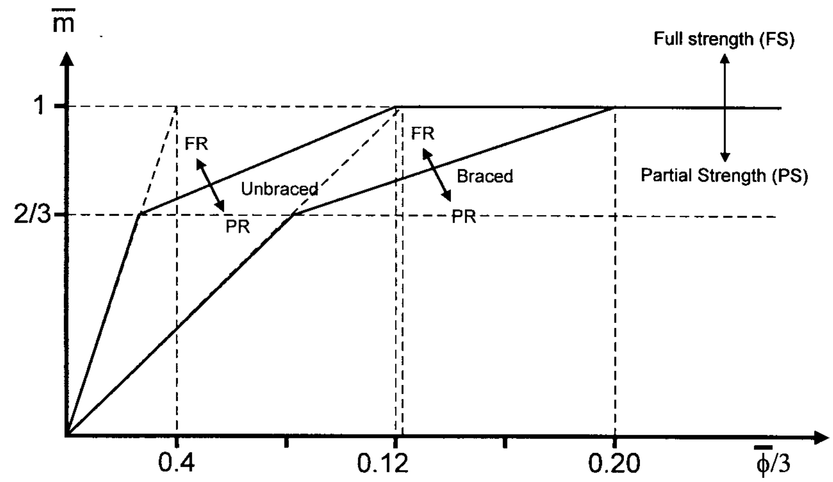

FIGURE 23.3: Normalized moment-rotation curves and connection classification. (After Eurocode 3, Design of Steel Structures, Part 1: General Rules and Rules for Buildings, ENV 1993-1-1: 1992, Comite Europeen de Normalisation (CEN), Brussels, 1992.)

In Figure 23.3, the vertical axis represents the ratio ($\overline{m}$) of the moment capacity of the connection ($M_{u,\mathrm{conn}}$) to the nominal plastic moment capacity ($M_{p,\mathrm{beam}} = Z_x F_y$) of the steel beam framing into it. As noted above, if this ratio is less than one then the connection is considered partial strength (PS); if it is equal or greater than one, then it is classified as a full strength (FS) connection. The horizontal axis is normalized to the end rotation of the framing beam assuming simple supports at the beam ends (θ_{ss}). This rotation depends, of course, on the loading configuration and the level of loading. Generally a factored distributed gravity load (w_u) and linear elastic behavior up to the full plastic capacity are assumed ($\theta_{ss} = w_u L_{\mathrm{beam}^3}/24EI_{\mathrm{beam}}$). The resulting reference rotation ($\overline{\phi} = M_p L/EI$), based on a M_p of $w_u L^2/8$, is $M_p L/(3EI) = \overline{\phi}/3$. It should be noted that the connection rotation is normalized with respect to the properties of the beam and not the column and that this normalization is meaningful only in the context of gravity loads. The column is assumed to be continuous and part of a strong column–weak beam system. For gravity loads its stiffness and strength are considered to contribute little to the connection behavior. This assumption, of course, does not account for panel zone flexibility which is important in many types of FS connections.

The non-dimensional format of Figure 23.3 is important because the terms partially restrained (PR) and full restraint (FR) can only be defined with respect to the stiffness of the framing members. Thus, a FR connection is defined as one in which the ratio (α) of the connection stiffness (k_{ser}) to the stiffness of the framing beam ($EI_{\mathrm{beam}}/L_{\mathrm{beam}}$) is greater than some value. For unbraced frames the recommended value ranges from 18 to 25, while for braced frames they range from 8 to 12. Figure 23.3 shows the limits chosen by the Eurocode, which are 25 for the unbraced case and 8 for the braced case [15]. These ranges have been selected based on stability studies that indicate that the global buckling load of a frame with PR connections with stiffnesses above these limits is decreased by less than 5% over the case of a similar frame with rigid connections. The large difference between the braced and unbraced values stems from the P-Δ and P-δ effects on the latter. PR connections are defined as those having α ranging from about 2 up to the FR limit. Connections with α less than 2 are regarded as pinned.

23.3 PR Composite Connections

Conventional steel design in the U.S. separates the design of the gravity and lateral load resisting systems. For gravity loads the floor beams are assumed to be simply supported and their section properties are based on assumed effective widths for the slab (AISC Specification I3.1 [2]) and a simplified definition of the degree of interaction (Lower Bound Moment of Inertia, Part 5 [3]). The simple supports generally represent double angle connections or single plate shear connections to the column flange. For typical floor beam sizes, these connections, tested without slabs, have shown low initial stiffness ($\alpha < 4$) and moment capacity ($M_{u,\mathrm{conn}} < 0.1 M_{p,\mathrm{beam}}$) such that their effect on frame strength and stiffness can be characterized as negligible. In reality when live loads are applied, the floor slab will contribute to the force transfer at the connection if any slab reinforcement is present around the column. This reinforcement is often specified to control crack widths over the floor girders and column lines and to provide structural integrity. This results in a weak composite connection as shown in Figure 23.4. The effect of a weak PR composite connection on the behavior under gravity loads is shown in Example 23.1.

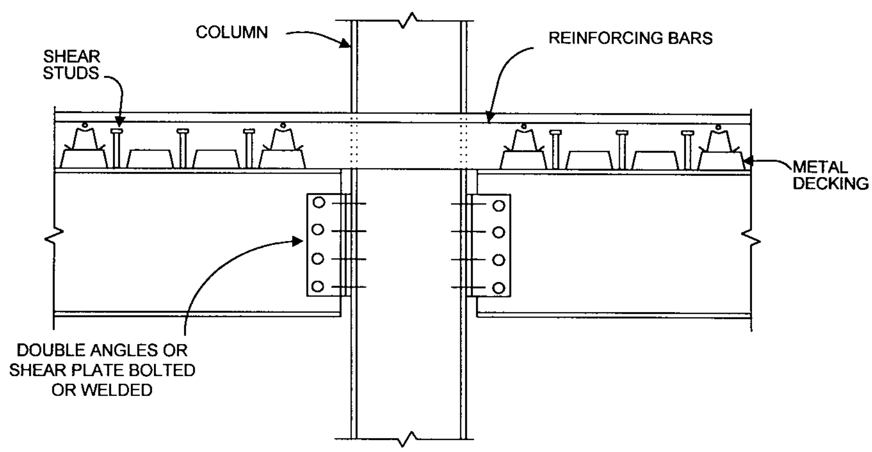

FIGURE 23.4: Weak PR composite connection.

EXAMPLE 23.1: Effect of a Weak Composite Connection

Consider the design of a simply-supported composite beam for a DL = 100 psf and a LL = 80 psf. The span is 30 ft and the tributary width is 10 ft. For this case the factored design moment (M_u) is 3348 kip-in. and the required nominal moment (M_n) is 3720 kip-in. From the AISC LRFD

Manual [3] one can select an A36 W18x35 composite beam with 92% interaction (PNA $= 3$, $\phi M_p =$ 3720 kip-in., and $I_{LB} = 1240$ in.^{4}). The W18x35 was selected based on optimizing the section for the construction loads, including a construction LL allowance of 20 psf. The deflection under the full live load for this beam is 0.4 in., well below the 1 in. allowed by the L/360 criterion. Thus, this section looks fine until one starts to check stresses. If we assume that all the dead load stresses from 1.2DL, which are likely to be present after the construction period, are carried by the steel beam alone, then:

$$\sigma_{DL,\text{steel alone}} = M_{DL}/S_x = 1620 \text{ kip-in. }/57.6 \text{ in.}^3 = 28.1 \text{ ksi}$$

The stresses from live loads are then superimposed, but on the composite section. For this section $S_{eff} = 91.9$ in.^{3}, so the additional stress due to the arbitrary point-in-time (APT) live load (0.5LL) is:

$$\sigma_{LL(APT)} = M_{LL(APT)}/S_{eff} = 540 \text{ kip-in.}/91.9 \text{ in.}^3 = 5.9 \text{ ksi}$$

Thus, the total stress (σ_{APTl}) under the APT live load is:

$$\sigma APT = \sigma_{DL,\text{steel alone}} + \sigma_{LL(APT)} = 28.1 + 5.9 = 34.0 \text{ ksi}$$

Under the full live load ($1.0LL$), the stresses are:

$$\sigma_{APT} = \sigma_{DL,\text{steel alone}} + 2\sigma_{LL(APT)} = 28.1 + 11.8 = 39.9 \text{ ksi } > F_y = 36 \text{ ksi}$$

Thus, the beam has yielded under the full live loads even though the deflection check seemed to imply that there were no problems at this level. The current LRFD provisions do not include this check, which can govern often if the steel section is optimized for the construction loads.

Let us investigate next what the effect of a weak PR connection, similar to that shown in Figure 23.3, will be on the service performance of this beam. Assume that the beam frames into a column with double web angles connection and that four #3 Grade 60 bars have been specified on the slab to control cracking. These bars are located close enough to the column so that they can be considered part of the section under negative moment. The connection will be studied using the very simple model shown in Figure 23.5. In this model all deformations are assumed to be concentrated in an area very close to the connection, with the beam and column behaving as rigid bodies. The reinforcing bars are treated as a single spring (K_{bars}) while the contribution to the bending stiffness of the web angles (K_{shear}) is ignored. The connection is assumed to rotate about a point about 2/3 of the depth of the beam.

Assuming that the angles and bolts can carry a combination of compression and shear forces without failing, at ultimate the yielding of the slab reinforcement will provide a tensile force (T) equal to:

$$T = \left(4 \text{ bars } * 0.11 \text{ in.}^2/\text{ bar } * 60 \text{ ksi}\right) = 26.4 \text{ kips}$$

This force acts an eccentricity (e) of at least:

$$e = \text{ two-thirds of the beam depth } + \text{ deck rib height} = 12\text{in.} + 3 \text{ in.} = 15 \text{ in.}$$

This results in a moment capacity for the connection ($M_{u,\text{conn}}$) equal to:

$$M_{u,\text{conn}} = T * e = 26.4 * 15 = 396 \text{ kip-in.}$$

The capacity of the beam ($M_{p,\text{beam}}$) is:

$$M_{p,\text{beam}} = Z_x * F_y = 66.5 \text{ in.}^3 * 36 \text{ ksi } = 2394 \text{ kip-in.}$$

Thus, the ratio ($\overline{m}$) of the connection capacity to the steel beam capacity is:

$$\overline{m} = 396/2394 * 100 \approx 17\%$$

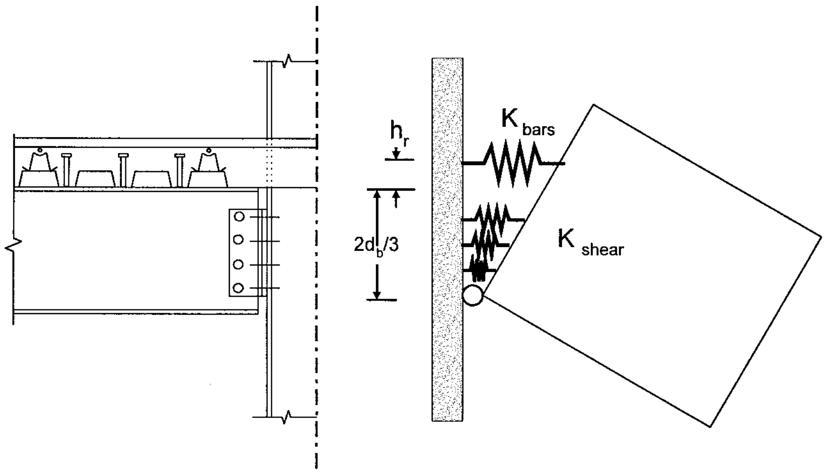

FIGURE 23.5: Simple mechanistic connection model.

If we assume that (1) the bars yield and transfer most of their force over a development length of 24 bar diameters from the point of inflection, (2) the strain varies linearly, and (3) the connection region extends for a length equal to the beam depth (18 in.), then the slab reinforcement can be modeled by a spring (K_{bars}) equal to:

$$K_{\text{bars}} = EA/L = \left(30{,}000 \text{ ksi } * 0.44 \text{ in.}^2\right)/(18 \text{ in.}) = 733.3 \text{ kips/in.}$$

Yield will be achieved at a rotation (θ_y) equal to:

$$\begin{aligned} \theta_y &= \left(T/\left(K_{\text{bars}} * e\right)\right) = \left(26.4 \text{ kips}/\left(733 \text{ kips/in. } \times 15 \text{ in.}\right)\right) \\ &= 0.0024 \text{ radians or } 2.4 \text{ milliradians} \end{aligned}$$

The connection stiffness (K_{ser}) can be approximated as:

$$K_{\text{ser}} = M_{u,\text{conn}}/\theta_y = 396 \text{ kip-in. }/0.0024 \text{ radians } = 165{,}000 \text{ kip-in./radian}$$

Assuming that the beam spans 30 ft, the beam stiffness is:

$$K_{\text{beam}} = EI_{\text{beam}}/L_{\text{beam}} = \left(30{,}000 \text{ ksi } * 510 \text{ in.}^4/360 \text{ in.}\right) = 42{,}500 \text{ kip-in./radian}$$

Thus, the ratio of connection to beam stiffness (α) is:

$$\alpha = K_{\text{ser}}/K_{\text{beam}} = 165{,}000/42{,}500 = 3.9$$

The relatively low values of α and $\overline{m}$ obtained for this connection, even assuming the non-composite properties in order to maximize α and $\overline{m}$, would seem to indicate that this connection will have little effect on the behavior of the floor system. This is incorrect for two reasons. First, the rotations (0.0024 radian) at which the connection strength is achieved are within the service range, and thus much of the connection strength is activated earlier than for a steel connection. Second, the composite connections only work for live loads and thus provide substantial reserve capacity to the system. The moments at the supports ($M_{PR\text{ conn}}$) due to the presence of these weak connections for the case of a uniformly distributed load (w) are:

$$M_{PR\text{ conn}} = wL^2/12 * 1/\left(1 + 2/\alpha\right) = wL^2/18.2$$

For the case of w being the APT live load, the moment is 238 kip-in., while for the case of the full live load it is 476 kip-in. This reduces the moments at the centerline from 540 kip-in. to 302 kip-in. for the APT live load and from 1080 kip-in. to 604 kip-in. for the full live load. The maximum additional stress is 6.6 ksi under full LL loads, so no yielding will occur. Thus, if a significant portion of the beam's capacity has been used up by the dead loads, a weak composite connection can prevent excessive deflections at the service level.

The connection illustrated in Figure 23.4 is one of the weakest variations possible when activating composite action. Figures 23.6 through 23.8 show three other variations, one with a seat angle, one with an end plate (partial or full), and one with a welded plate as the bottom connection. As compared with the simple connection in Figure 23.4, both the moment capacity and the initial stiffness of these latter connections can be increased by more slab steel, thicker web angles or end plates, and friction bolts in the seat and web connections. The selection of a bolted seat angle, end plate, or welded plate will depend on the amount of force that the designer wants to transfer at the connection and on local construction practices.

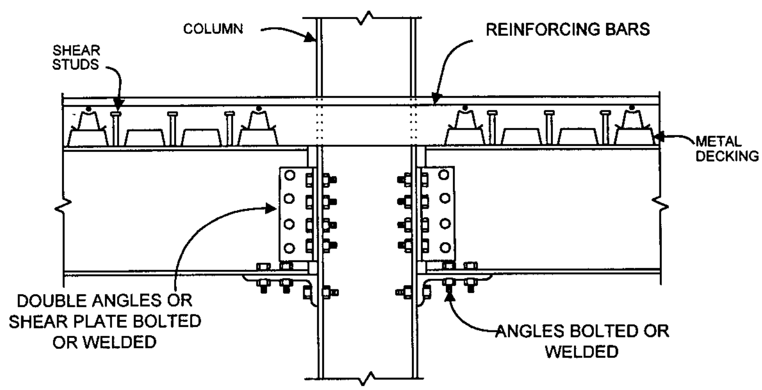

FIGURE 23.6: Seat angle composite connection.

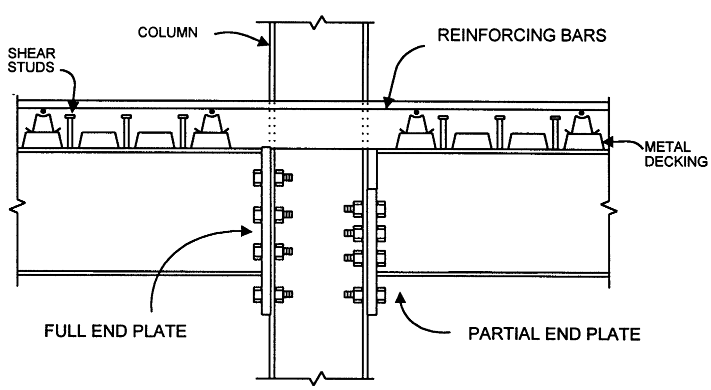

FIGURE 23.7: End plate composite connection.

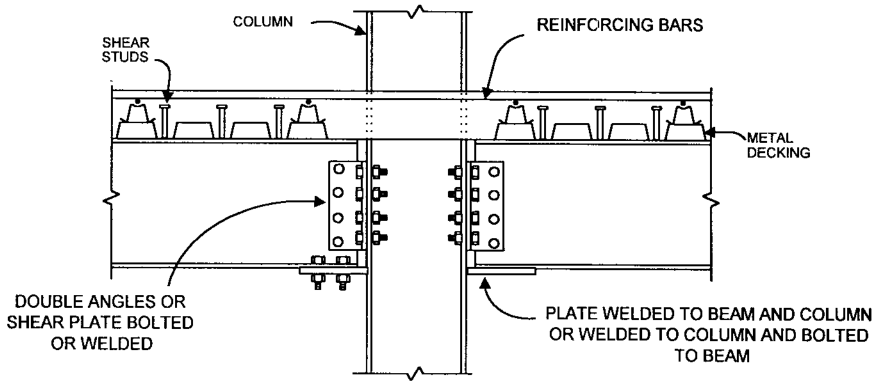

FIGURE 23.8: Welded bottom plate composite connection.

The behavior of these connections under gravity loads (negative moments) should be governed by gradual yielding of the reinforcing bars, and not by some brittle or semi-ductile failure mode. Examples of these latter modes are shear of the bolts and local buckling of the bottom beam flange. Both modes of failure are difficult to eliminate at large deformations due to the strength increases resulting from strain hardening of the connecting elements. The design procedures to be proposed here for composite PR connections intend to insure very ductile behavior of the connection to allow redistribution of forces and deformations consistent with a plastic design approach. Therefore, the intent in design will be to delay but not eliminate all brittle and semi-brittle modes of failure through a capacity design philosophy [22].

For the connections shown in Figures 23.6 through 23.8, if the force in the slab steel at yielding is moderate, it is likely that the bolts in a seat angle or a partial end plate will be able to handle the shear transfer between the column and the beam flanges. If the forces are high, an oversized plate with fillet welds can be used to transfer these forces. The connections in Figures 23.6 and 23.7 will probably be true PR/PS connections, while that in Figure 23.8 will likely be a PR/FS connection. In the latter case it is easy to see that considerable strength and stiffness can be obtained, but there are potential problems. These include the possibility of activating other less desirable failure mechanisms such as web crippling of the column panel zone or weld fracture.

The behavior of these connections under lateral loads that induce moment reversals (positive moments) at the connections should be governed by gradual yielding of the bottom connection element (angle, partial end plate, or welded plate). Under these conditions the slab can transfer very large forces to the column by bearing if the slab contains reinforcement around the column in the two principal directions. In this case, brittle failure modes to avoid include crushing of the concrete and buckling of the slab reinforcement.

The composite connections discussed here provide substantial strength reserve capacity, reliable force redistribution mechanisms (i.e., structural integrity), and ductility to frames. In addition, they provide benefits at the service load level by reducing deflection and vibration problems. Issues related to serviceability of structure with PR frames will be treated in the section on design of composite connections in braced frames.

23.4 Moment-Rotation (M-θ) Curves

As noted earlier, a prerequisite for design of frames incorporating PR connections is a reliable knowledge of the M-θ curves for the connections being used. There are at least four ways of obtaining them:

1. From experiments on full-scale specimens that represent reasonably well the connection configuration in the real structure [21]. This is expensive, time-consuming, and not practical for everyday design unless the connections are going to be reused in many projects.
2. From catalogs of M-θ curves that are available in the open literature [6, 16, 20, 27]. As discussed elsewhere [7, 22], extreme care should be used in extrapolating from the equations in these databases since they are based mostly on tests on small specimens that do not properly model the boundary conditions.
3. From advanced analysis, based primarily on detailed finite element models of the connection, that incorporate all pertinent failure modes and the non-linear material properties of the connection components.
4. From simplified models, such as that shown in Figure 23.5, in which behavioral aspects are lumped into simple spring configurations and other modes of failure are eliminated by establishing proper ranges for the pertinent variables.

Ideally M-θ curves for a new type of connection should be obtained by a combination of experimentation and advanced analysis. Simplified models can then be constructed and calibrated to other tests for similar types of connections available in the literature. For the composite connections shown in Figure 23.6, which will be labeled PR-CC, Leon et al. [23] followed that approach. They developed the following M-θ equation for these connections under negative moment for rotations less than 20 milliradians:

$$M^{-} = C1 * \left(1 - e^{(-C2*\theta)}\right) + C3 * \theta \tag{23.1}$$

where

$C1 \;=\; 0.1800 * \left[\left(4 * A_{rb} * F_{yrb}\right) + \left(0.857 * A_{sL} * F_{yL}\right)\right] * (d + Y3)$
$C2 \;=\; 0.7750$
$C3 \;=\; 0.0070 * (A_{sL} + A_{wL}) * (d + Y3) * F_{yL}$
$\theta \;=\;$ relative rotation (milliradians)
$A_{wL} \;=\;$ area of web angles resisting shear (in.^{2})
$A_{sL} \;=\;$ area of seat angle leg (in.^{2})
$A_{rb} \;=\;$ effective area of slab reinforcement (in.^{2})
$d \;=\;$ depth of steel beam (in.)
$Y3 \;=\;$ distance from top of steel shape to center of slab force (in.)
$F_{yL} \;=\;$ yield stress of seat and web angles (ksi)
$F_{yrb} \;=\;$ yield stress of slab reinforcement (ksi)

Since these connections will have unsymmetric M-θ characteristics due to presence of the concrete slab, the following equation was developed for these connections under positive moments for rotations less than 10 milliradians:

$$M^{+} = C1 * \left(1 - e^{(-C2*\theta)}\right) + (C3 + C4) * \theta \tag{23.2}$$

where

$C1 \;=\; 0.2400 = *[(0.48 * A_{Wl}) + A_{Sl}] * (d + Y3) * F_{Yl}$
$C2 \;=\; 0.0210 * (d + Y3/2)$
$C3 \;=\; 0.0100 * (A_{wL} + A_{sL}) * (d + Y3) * F_{yL}$
$C4 \;=\; 0.0065 * A_{wL} * (d + Y3) * F_{yL}$

For preliminary design it may be necessary to model the connections as bi-linear springs only, characterized by a service stiffness (k_{conn}), an ultimate strength ($M_{u,\text{conn}}$), and hardening stiffness

(k_{ult}). Simplified expressions for these are as follows:

$$K_{\mathrm{conn}} = 85\left[\left(4A_{rb}F_{yr}\right)+\left(A_{wL}F_{yL}\right)\right](d+Y3) \tag{23.3}$$

$$M_{u,\mathrm{conn}} = 0.245\left[\left(4A_{rb}F_{yr}\right)+\left(A_{wL}F_{yL}\right)\right](d+Y3) \tag{23.4}$$

$$K_{\mathrm{ult}} = 12.2\left[\left(4A_{rb}F_{yr}\right)+\left(A_{wL}F_{yL}\right)\right](d+Y3) \tag{23.5}$$

For a final check, it is desirable to model the entire response using Equations 23.1 and 23.2 or some piecewise linear version of them. The author has proposed a tri-linear version for Equation 23.1 for which the three breakpoints are defined as [5]:

$\theta 1$ = the rotation at which the tangent stiffness reaches 80% of its original value
$M1$ = moment corresponding to $\theta 1$
$\theta 2$ = the rotation at which the exponential term of the connection equations $\left(e^{-C2*q}\right)$ is equal to 0.10
$M2$ = moment corresponding to $\theta 2$
$\theta 3$ = equal to 0.020 radians, close to the maximum rotation required for this type of connection
$M3$ = moment corresponding to $\theta 3$

It is necessary in this case to differentiate Equation 23.1 and set θ equal to zero to find an initial stiffness, and then backsolve for the rotation corresponding to 80% of that initial stiffness. All the examples in this chapter are worked out in English units because metric versions of Equations 23.1 through 23.5 have not yet been properly tested.

EXAMPLE 23.2: Moment-Rotation Curves

Figure 23.9b shows the complete M-θ curve for the composite PR connection shown in Figure 23.9a. The values shown in Figure 23.9b were taken directly from substituting into Equations 23.1 through 23.4. The shaded squares show the breakpoints for the trilinear curves described in the previous section. The trilinear curve for positive moment was derived by using the same definitions as for negative moments but limiting the rotations to 10 milliradians, the limit of applicability of Equation 23.2. Tables for the preliminary and final design of this type of connection are given in a recently issued design guide [26].

The M-θ curves shown in Figure 23.9b are predicated on a certain level of detailing and some assumptions regarding Equations 23.1 through 23.5, including the following:

1. In Equations 23.1 and 23.2, the area of the seat angles (A_{sL}) shall not be taken as more than 1.5 times that of the reinforcing bars (A_{rb}).
2. In Equations 23.1 and 23.2, the area of the web angles (A_{wL}) resisting shear shall not be taken as more than 1.5 times that of one leg of the seat angle (A_{sL}) for A572 Grade 50 steel and 2.0 for Grade A36.
3. The studs shall be designed for full interaction and all provisions of Chapter I of the LRFD Specification [2] shall be met.
4. All bolts, including those to the beam web, shall be slip-critical and only standard and short-slotted holes are permitted.
5. Maximum nominal steel yield strength shall be taken as 50 ksi for the beam and 60 ksi for the reinforcing bars. Maximum concrete strength shall be taken as 5 ksi.
6. The slab reinforcement should consist of at least six longitudinal bars placed symmetrically within a total effective width of seven column flange widths. For edge beams the steel should be distributed as symmetrically as possible, with at least 1/3 of the total on the edge side.

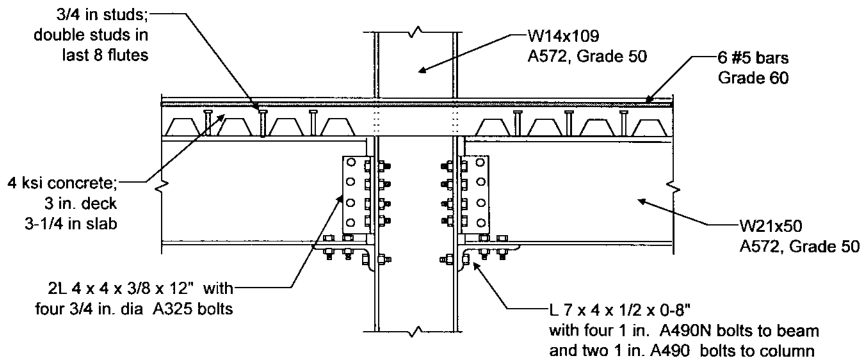

(a) Details of Type I PR-CC

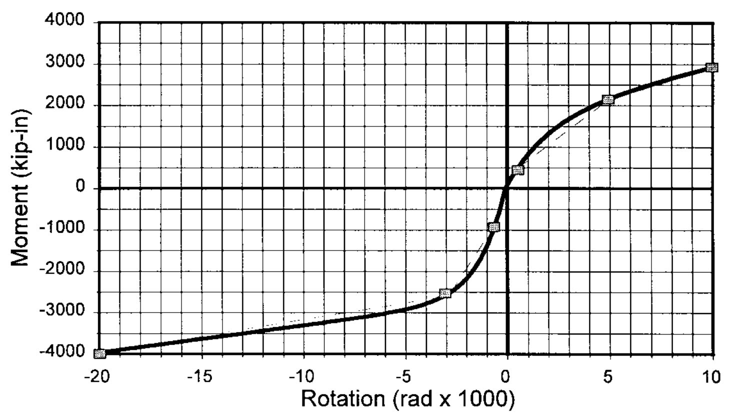

(b) Moment-rotation curve

FIGURE 23.9: Typical PR-CC connection and its moment-rotation curves.

7. Transverse reinforcement, consistent with a strut-and-tie model, shall be provided. In the limit the amount of transverse reinforcement will be equal to that of the longitudinal reinforcement.
8. The maximum bar size allowed is #6 and the transverse reinforcement should be placed below the top of the studs whenever possible.
9. The slab steel should extend for a distance given by the longest of $L_b/4$ or 24 bar diameters past the assumed inflection point. At least two bars should be carried continuously across the span.
10. All splices and reinforcement details shall be designed in accordance with ACI 318-95 [1].
11. Whenever possible the space between the column flanges shall be filled with concrete. This aids in transferring the forces and reduces stability problems in the column flanges and web.

These detailing requirements must be met because the analytical studies used to derive Equations 23.1 and 23.2 assumed this level of detailing and material performance. Only Item 11 is optional but strongly encouraged for unbraced applications Compliance with these requirements means that extensive checks for the ultimate rotation capacity will not be needed.

23.5 Design of Composite Connections in Braced Frames

The design of PR-CCs requires that the designer carefully understand the interaction between the detailing of the connection and the design forces. Figure 23.10 shows the moments at the end and centerline, as well as the centerline deflection, for the case of a prismatic beam under a distributed load with two equal PR connections at its ends. The graph shows three distinct, almost linear zones for each line; two horizontal zones at either end and a steep transition zone between α of 0.2 and 20. Note that the horizontal axis, which represents the ratio of the connection to the beam stiffness, is logarithmic. This means that relatively large changes in the stiffness of the connection have a relatively minor effect. For example, consider the case of a beam with PR-CCs with a nominal α of 10. This gives moments of $wL^2/13.2$ at the end and $wL^2/20.3$ at centerline, with a corresponding deflection of 1.67 $wL^4/384EI$. If the service stiffness (k_{ser}) for this connection is underestimated by 25% ($\alpha = 7.5$) these values change to $wL^2/13.6$, $wL^2/19.4$, and $1.84wL^4/384EI$. These represent changes of 3.0%, 4.4%, and 10%, respectively, and will not affect the service or ultimate performance of the system significantly. This is why the relatively large range of moment-rotation behavior, typical of PR connections and shown schematically in Figure 23.2, does not pose an insurmountable problem from the design standpoint.

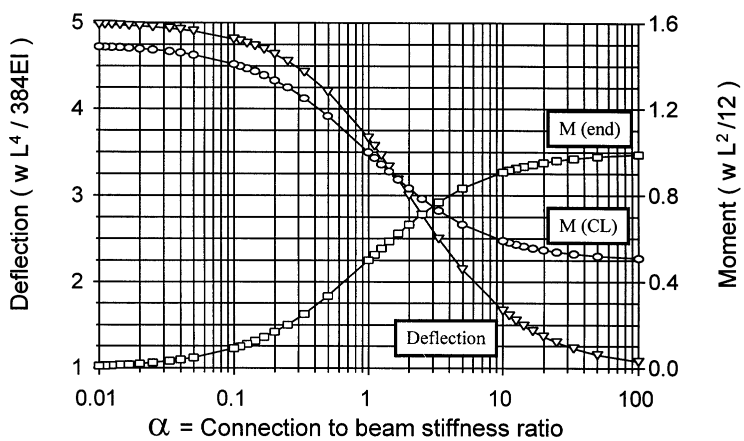

FIGURE 23.10: Moments and deflections for a prismatic beam with PR connections under a distributed load.

For continuous composite floors in braced frames, where the floor system does not participate in resisting lateral loads, the design for ultimate strength can be based on elastic analysis such as that shown in Figure 23.10 or on plastic collapse mechanisms. If elastic analysis is used, it is important to recognize that both the bending resistance and the moments of inertia change from regions of negative to positive moments. The latter effect, which would be important in elastic analysis, is not considered in the calculations for Figure 23.10. In the case of the fixed ended beam with full strength connections (FR/FS), elastic analysis ($\alpha = \infty$ in Figure 23.10) results in the maximum force corresponding to the area of lesser resistance. This is why it would be inefficient to design continuous composite beams with FR connections from the strength standpoint. As the connection stiffness is reduced, the ratio of the moment at the end to the centerline begins to decrease. From Figure 23.10, for a prismatic beam, the optimum connection stiffness is found to be around $\alpha = 3$, where the moments at the ends and middle are equal ($wL^2/16$). This indicates that it takes relatively little restraint to get a favorable distribution of the loads. If the effect of the changing moments of inertia is included, as it should for the case of composite beams, the sloping portions of the moment curves in Figure 23.10 will move to the right. For this case, the optimum solution will not be at the intersection of the M(end) and M (CL) lines but at the location where the ratio of $M_{p,ci}/M_{p,b}$ equals M(end)/ M (CL). Preliminary studies indicate that the optimum connection stiffness for composite beams is generally found to be still around α of 3 to 6. This indicates that it takes relatively little restraint to get a favorable distribution of the loads. This type of simple elastic analysis, however, cannot account for the fact that the connection M-θ curves are non-linear and thus will not be useful in the analysis of PR/PS connections such as PR-CCs.

Design of continuous beams with PR connections can be carried out efficiently by using plastic analysis. The collapse load factor for a beam (λ_b) with a plastic moment capacity $M_{p,b}$ at the center, and connection capacities $M_{p,c1}$, and $M_{p,c2}(M_{p,c1} > M_{p,c2})$ at its ends, can be written as:

$$\lambda_b = \frac{d}{\left(PL \text{ or } wL^2\right)}\left(aM_{p,c1} + bM_{p,c2} + cM_{p,b}\right) \tag{23.6}$$

where the coefficients a, b, c, and d are given in Table 23.1, P and w are the point and distributed loads, and L is the beam length, respectively. For Load Cases 1 through 4, the spacing between the loads is assumed equal.

TABLE 23.1 Values of Constants in Equation 23.7 for Different Loading Configurations

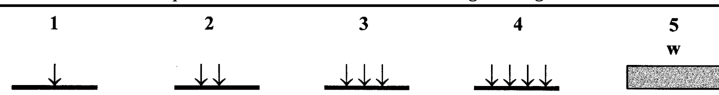

	Connection relationship											
	$M_{p,c1} = M_{p,c2}$				$M_{p,c1} > M_{p,c2}$				$M_{p,c2} = 0$			
	a	b	c	d	a	b	c	d	a	b	c	d
1	1	0	1	4	1	1	2	2	1	0	2	2
2	1	0	1	3	1	2	3	1	1	0	3	1
3	1	0	1	2	1	1	2	1	1	0	2	1
4	1	0	1	$\frac{5}{3}$	2	3	5	$\frac{5}{12}$	2	0	5	$\frac{5}{12}$
5	1	0	1	8					1	0	$\frac{L}{x}$	$\frac{2L}{L-x}$

For the case of a distributed load (Load Case 5) with unequal end connections ($M_{p,c1} > M_{p,c2}$), it is not possible to write a simple expression in the form of Equation 23.6 because the solution requires locating the position of the center hinge. For the case of $M_{p,c2} = 0$, the position can be calculated by:

$$x = \frac{M_{p,b}}{M_{p,c1}} L \left\{\sqrt{1 + \frac{M_{p,c1}}{M_{p,b}}} - 1\right\} \tag{23.7}$$

If plastic analysis is used, it is important to recognize that the flexural strength changes from the area of negative ($M_{p,c1}$ and $M_{p,c2}$) to positive moment ($M_{p,b}$), and that the ratio of $M_{p,ci}/M_{p,b}$ will often be 0.6 or less.

For the service limit state, it is important again to recognize that the results shown in Figure 23.10 are valid only for a prismatic beam. In reality a continuous composite beam will be non-prismatic, with the positive moment of inertia of the cross-section (I_{pos}) often being 1.5 to 2.0 times greater than the negative one (I_{neg}). It has been suggested that an equivalent inertia (I_{eq}), representing a weighted average, should be used [5]:

$$I_{\mathrm{eq}} = 0.4 I_{\mathrm{neg}} + 0.6 I_{\mathrm{pos}} \tag{23.8}$$

The effect of accounting for the non-prismatic characteristics of the beam is far more important in calculating deflections than in calculating the required flexural resistance. For calculating deflections of beams with equal PR connections at both ends, the following expression has been proposed [5]:

$$\delta_{PR} = \delta_{FR} + \frac{C_\theta \theta_{\mathrm{sym}} L}{4} \tag{23.9}$$

where

δ_{PR} = the deflection of the beam with partially restrained connections
δ_{FR} = the deflection of the beam with fixed-fixed connections
C_θ = a deflection coefficient
θ_{sym} = the service load rotation corresponding to a beam with both connections equal to the stiffest connection present

When the beam has equal connection stiffnesses, C_θ equals one. Values for the constant C_θ in Equation 23.9 are given in Table 23.2 for some common loading cases.

TABLE 23.2 Constants for Deflection Calculations by Equation 23.9

	$1/(1+\alpha)$								
K_b/K_a	0.9	0.8	0.7	0.6	0.5	0.4	0.3	0.2	0.1
1	1	1	1	1	1	1	1	1	1
0.9	1.05	1.04	1.04	1.03	1.03	1.02	1.02	1.01	1.01
0.8	1.11	1.09	1.08	1.07	1.05	1.04	1.03	1.02	1.01
0.7	1.18	1.15	1.13	1.11	1.09	1.07	1.05	1.03	1.02
0.6	1.27	1.22	1.18	1.15	1.12	1.09	1.07	1.04	1.02
0.5	1.39	1.31	1.25	1.20	1.16	1.12	1.08	1.05	1.03
0.4	1.54	1.41	1.32	1.25	1.20	1.15	1.10	1.07	1.03
0.3	1.76	1.55	1.41	1.32	1.24	1.18	1.12	1.08	1.04
0.2	2.09	1.72	1.52	1.39	1.29	1.21	1.15	1.09	1.04
0.1	2.63	1.97	1.66	1.47	1.34	1.25	1.17	1.10	1.05
0	3.70	2.32	1.83	1.57	1.40	1.28	1.19	1.12	1.05

Note: K_b = stiffness of the less stiff connection; K_a = stiffness of the stiffer connection; $1/(1+\alpha/2) = M_{\mathrm{conn,PR}}/M_{\mathrm{conn,fixed}}$ and; $\alpha = EI/(K_a L)$.

The value of θ_{symm} is given by:

$$\theta_{\mathrm{symm}} = \frac{M_{\mathrm{FEM}}}{K_{\mathrm{ser}} + \left(1 + \frac{2}{\alpha}\right)}$$

where

M_{FEM} = the fixed end moment
K_{conn} = the stiffness of the connection
α = the ratio of the connection to the beam stiffness

The effect of partially restrained connections on floor vibrations is an area that has received comparatively little attention. Figure 23.11 shows the changes in natural frequency for a prismatic beam with a distributed load as the stiffness of the end connections change. The connections at both ends are assumed equal and the connection stiffness is assumed to be linear. The natural frequency (f_n, Hz) is given by:

$$f_n = \frac{K_n^2}{2\pi}\sqrt{\frac{EI}{mL^4}} \tag{23.10}$$

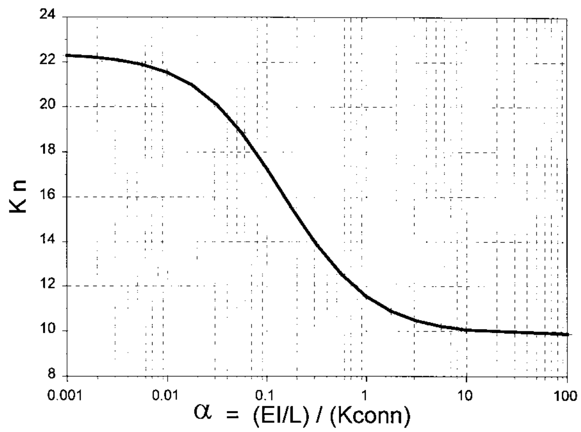

FIGURE 23.11: First natural frequency of vibration for a beam with PR connections.

where m is the mass per unit length, L is the length, and EI is the stiffness of the beam.

Generally m is taken as the distributed load (w) given by the dead plus 25% of the live loads and divided by the acceleration of gravity (g = 386 in./s^2). Limit values of K_n range from π^2 for the simply supported case to $(1.5\pi)^2$ for the fixed case.

EXAMPLE 23.3:

Design a continuous floor system in a braced frame. The system will consist of a three-span girder with a total length of 96 ft, and will be designed for dead loads of 80 psf and live loads of 100 psf. The reduced live loads will be taken as 60 psf. This girder supports floor beams spanning 28 ft in the perpendicular direction every 8 ft, for a total of three point loads per span. In addition to the distributed loads described above, the interior span will support equipment weighing 15 kips, to be installed before the slab is cast (Figure 23.12). Cambering will be provided to offset all dead loads, including the equipment. The connections to the exterior columns will be assumed as pinned since an overhang would be required to anchor the slab reinforcement. The steel will be A572 Grade 50 and a 3-1/4 in. lightweight concrete slab ($f'_c = 4$ ksi) on 3 in. metal deck (Y2 = 4.5 in.) will be assumed.

The construction dead loads are assumed as 60 psf and the construction live loads are taken as 15 psf. The design construction load, assuming distributed loads, is:

$$\begin{aligned} w_{u,\text{const}} &= [1.2(0.06) + 1.6(0.015)]\,(28 \text{ ft.}) = 2.69 \text{ k/ft} \\ M_{u,\text{const}} &= wL^2/8 = (2.69)(32)^2/8 = 344 \text{ k-ft} = 4129 \text{ kip-in.} \\ Z_x &= 4129/(0.9 \times 50) = 91.8 \text{ in.}^3 \end{aligned}$$

Assuming that the beam will be supported laterally during the construction phase, the most economical steel section would be a W21x44 ($Z_x = 95.4$ in.^{3}). For the ultimate strength limit state, assuming three point loads at the location of the floor beams, for the interior span:

$$\begin{aligned} P_{u,} &= [1.2(0.08) + 1.6(0.06)]\,(28 \text{ ft.})(8 \text{ ft.}) + 1.2(15 \text{ kips}) = 61.0 \text{ kips} \\ \phi M_{u,} &= 15P_uL/32 = 15(61.0)(32)/32 = 915 \text{ k-ft} = 10{,}980 \text{ kip-in.} \end{aligned}$$

For the ultimate strength limit state in the exterior spans:

$$P_{u,} = [1.2(0.08) + 1.6(0.06)]\,(28 \text{ ft.})(8 \text{ ft.}) = 43.0 \text{ kips}$$

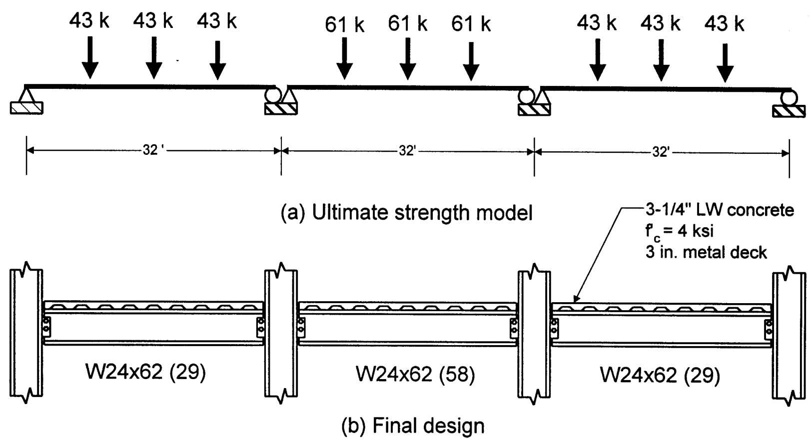

FIGURE 23.12: Design of composite floor system as simply supported beams (numbers in parenthesis are the number of shear studs).

$$\phi M_{u,} \quad = \quad 15 P_u L/32 = 15(61.0)(32)/32 = 645 \text{ k-ft } = 7{,}742 \text{ kip-in.}$$

If we assume typical current construction practice and design these girders as simply supported composite beams, for the ultimate load condition the section required will be a fully composite W24x55 (Y2 = 4.5 in. and $\sum Q_n = 810$ kips). Assuming $f_c' = 4$ ksi and 3/4 in. headed studs, 38 shear studs per half-span, or more than two studs per flute, will be needed. This is not a very efficient design, and thus a partially composite W24x62 will be a better choice ($\phi M_p = 930$ kip-ft with Y2 = 4.0 in. and $\sum Q_n = 598$ kips). This results in 29 studs per half-span or roughly two studs per flute.

The service load deflection in this case would be:

$$\begin{aligned}\delta \quad = \quad & 19PL^3/384EI = \left[19 \times (0.06 \times 28 \times 8) \times (32 \times 12)^3\right] / \\ & [384 \times 29000 \times 2180] = 0.595 \text{ in. } \approx L/640\end{aligned}$$

For the exterior spans, a W24x62 with the minimum amount of interaction (25%, or $M_p = 755$ kip-ft with Y2 = 4.0 in. and $\sum Q_n = 228$ kips) and 21 studs total will suffice.

If we were to provide a PR-CC such as the one shown in Figure 23.9, one could calculate its ultimate strength ($M_{u,\text{conn}}$), from Equation 23.4 as:

$$M_{u,\text{conn}} = 0.245 \left[\left(4 \times \left(6 \times 0.31 \text{ in.}^2\right) \times 60 \text{ ksi}\right) + (4.00 \times 50)\right] \times (21 + 4) = 3{,}959 \text{ kip-in.}$$

Note that the nominal capacity of the connection ($M_{u,\text{conn}} = 3{,}959$ kip-in.) has to be less than or equal to that of the steel beam $\phi(M_{p,b} = 4{,}293$ kip-in.) in order to insure that the hinging will not occur in the beam. The author has suggested [22] that a good starting point for the strength design is to assume that the connection will carry about 70 to 80% of $M_{p,b}$. For our case the ratio is 3,959/6,888 = 0.58 which is somewhat lower but reasonable because of the heavy dead loads.

For the interior span, from Equation 23.6 and assuming that $M_{p,c1} = M_{p,c2} = \phi M_{u,\text{conn}} = (0.9 \times 3959) = 3563$ kip-in., for a collapse load factor (λ_p) of 1.00:

$$\begin{aligned}1.00 \quad &= \quad \frac{(2)}{(61 \times 32 \times 12)} \left(3563 + \phi M_{p,b}\right) \\ \phi M_{p,b} \quad &= \quad 8149 \text{ kip-in.} = 679 \text{ kip-ft}\end{aligned}$$

For the exterior span, from Equation 23.6 and assuming that $M_{p,c1} = 0$ and $M_{p,c2} = \phi M_{u,\text{conn}} = (0.9 \times 3959) = 3563$ kip-in., for a collapse load factor (λ_p) of 1.00:

$$\begin{aligned} 1.00 &= \frac{(1)}{(43 \times 32 \times 12)} \left(3563 + 2\phi M_{p,b}\right) \\ \phi M_{p,b} &= 6474 \text{ kip-in.} = 540 \text{ kip-ft} \end{aligned}$$

The required strength can now be provided by a fully composite W21x44 ($\phi M_n = 683$ kip-in., and $\sum Q_n = 650$ kips or two studs per flute) and by a partially composite W21x44 ($\phi M_n = 564$ kip-in., and $\sum Q_n = 260$ kips or one studs per flute). Figure 23.13 shows the analysis model and the final design for this case, as well as the moment diagram for the case of DL + LL.

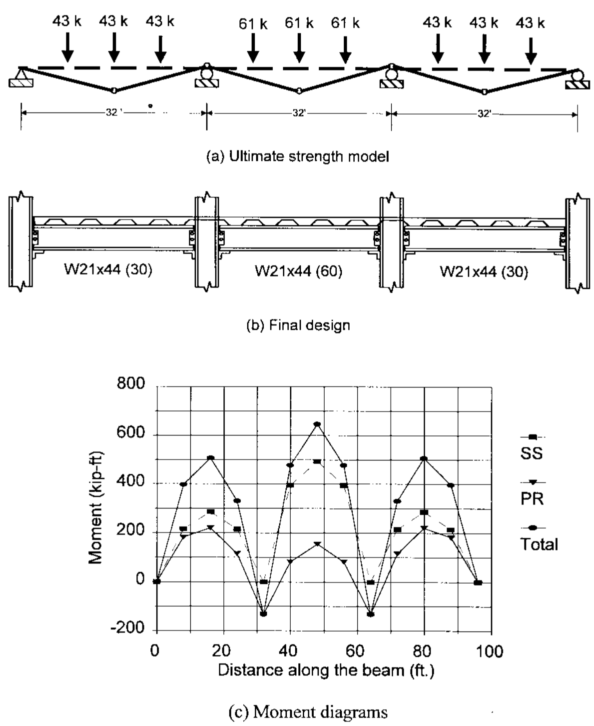

FIGURE 23.13: Continuous beam design with PR connections.

Figure 23.13c shows that the dead load moments are calculated on the simply supported structure (SS), while the live load ones are calculated on the continuous structure (PR). For calculation purposes, the moments of inertia were taken as 1699 in.^{4} for the interior span and 1399 in.^{4} for the exterior span, as per Equation 23.8. Figure 23.13c indicates that the maximum moment in the interior span at full service load is 647 kip-ft. This is close to the factored capacity of the section ($\phi M_n = 683$ kip-ft). Thus, careful attention should be paid to the stresses and deflections at service loads when using a plastic design approach since the latter does not consider construction sequence or the onset of yielding. In this case perhaps a W21x50 section, with the same number of studs, would be a more prudent design.

In computing the forces for the case of the PR system, the connection stiffness was calculated directly as a secant stiffness at 0.002 radian from Equation 23.1. The stiffness was 1.135×10^6 kip-in./rad, which is slightly lower than the 1.398×10^6 kip-in./rad given by Equation 23.3. The α for this connection is:

$$\alpha = \frac{K_{\text{ser}} L}{EI} = \frac{(1.135 \times 10^6)(32 \times 12)}{(29000)(1699)} = 8.84$$

This puts this PR connection near the middle of the PR range for unbraced frames and near the rigid case for the case of braced frames.

The deflection of the center span under the full live load is, from Equation 23.9:

$$\delta_{PR} = \frac{PL^3}{96EI} + \frac{C_\theta M_{FF} L}{4K_{\text{conn}}\left(1 + \frac{2}{\alpha}\right)} = 0.161 + 0.109 = 0.270 \text{ in.} \approx L/1500$$

This deflection is considerably less than that computed for the simply supported case even when a much larger section (W24x62) was used in the latter case. An idea of the effect of this PR connection can be gleaned from inspecting Figure 23.10. Although Figure 23.10 corresponds to a different case, the moment diagrams are not substantially different and thus a meaningful comparison can be made for the elastic case. From Figure 23.10, the difference in deflection between a simple support and a PR connection with $\alpha = 8.84$ is roughly a factor of 2.8 (5/1.8), while the difference in moment of inertia is only 1.28 (2180 in.^{4} / 1699 in.^{4}). In this example, the design was governed by strength and not deflections. However, this example clearly shows the impact of a PR connection in reducing floor deflections.

In addition to the strength calculation above, the design procedure requires that the following limit states and design criteria be satisfied (refer to Figure 23.9a for details):

1. Shear strength of the bolts attaching the seat angle to the beam (ϕV_{bolts}): The bolts have to be designed to transfer, through shear, a compressive force corresponding to 1.25 of the force (T_{slab}) in the slab reinforcement. The 1.25 factor accounts for the typical overstrength of the reinforcement, and intends to insure that the bolts will be able to carry a force consistent with first yielding of the slab steel. Assuming 1 in. diameter A490N bolts:

$$\begin{aligned}(\phi V_{\text{bolts}}) &= 1.25 T_{\text{slab}} = 1.25 F_y A_{\text{bars}} = 139.5 \text{ kips} \\ N\text{bolts} &= (\phi V_{\text{bolts}})/35.3 = 3.95 \cong 4 \text{ bolts (O.K.)}\end{aligned}$$

2. Bearing strength at the bolt holes (ϕR_n): The thickness of the angle will be governed by the required flexural resistance of the angle leg connecting to the beam flange in the case of a connection in an unbraced frame, where tensile forces at the bottom of the connection are possible. It will be governed by either bearing of the bolts or compressive yielding of the angle leg in the case of a connection in a braced frame. In this case:

$$\begin{aligned}\phi R_n &= \phi(2.4 d t F_u) = 0.75(2.4 \times 0.875 \times 0.5 \times 65) \\ &= 51.2 \text{ kips/bolt } > \phi V_{\text{bolts}}\text{, O.K.}\end{aligned}$$

3. Tension yield and rupture of the seat angle: This limit state is strictly applicable to the case of unbraced frames where pull-out of the angle under positive moments is possible. For the case of a connection in a braced frame, it is prudent to check the angle for yielding under compressive forces (ϕC_n) and possible buckling. The latter is never a problem given the short gage lengths, while the former is:

$$\phi C_n = \phi\left(A_g F_y\right) = 0.9 \times (8 \times 0.5) \times 50 = 180 \text{ kips } > \phi V_{\text{bolts}}\text{, O.K.}$$

4. Number and distribution of slab bars, including transverse reinforcement, to insure a proper strut-and-tie action at ultimate (see section following Example 23.2 for details).
5. Number and distribution of shear studs to provide adequate composite action (checked above as part of the flexural design).
6. Tension strength, including prying action, for the bolts connecting the beam to the column.
7. Shear capacity of the web angles.
8. Block shear capacity of the web angles.
9. Check for the need for column stiffeners

Limit states (6) through (9) can be checked following the current LRFD provisions, and the details will not be provided here. However, it should be clear from the few calculations shown above that the shear capacity of the bolts is the primary mechanism limiting the forces in the connection.

The structural benefits of using a PR-CC connection are clear from the results of this example. From the economic standpoint, for a PR-CC to be beneficial, the cost of the additional reinforcing bars and seat angle bars has to be offset by that of the additional studs and larger sections required for the simply supported case. In some instances the benefits may not be there from the economic standpoint, but the designer may choose to use PR-CCs anyway because of their additional redundancy and toughness.

In Example 23.3, the design was controlled by strength and thus it was relatively simple to calculate forces based on plastic analysis and proportion the connection based on a simplified model similar to that shown in Figure 23.5. Since deflections did not control the design, the connection stiffness did not play an appreciable role in the preliminary design. If serviceability criteria control the design, then the proportioning of the connection can start from Equation 23.3. In this case the analysis has to be iterative, since the value of the connection stiffness will affect the moment diagram and the deflection. For applications in braced frames, however, experience indicates that it is strength and not stiffness that governs the design. This is because the steel beam size is controlled by the construction loads if the typical unshored construction process is used. In general, the steel beam selected is capable of providing the required stiffness even if it is the minimum amount of interaction (25% is recommended by AISC and 50% by this author).

23.6 Design for Unbraced Frames

As noted earlier, the design of frames with PR connections requires that the effects of the non-linear stiffness and partial strength characteristics of the connections be incorporated into the analysis. From the practical standpoint, the main difference between the design of unbraced FR and PR frames is the contribution of the connections to the lateral drift. The designer thus needs to balance not just the stiffness of the columns and beams to satisfy drift requirements, but account for the additional contribution of the concentrated rotations at the connections. There are no established practical rules on the best distribution of resistance to drift between columns, beams, and connections for PR-CCs. Trial designs indicate that distributing them about equally is reasonable (i.e., 33% to the beams, columns, and connections, respectively), and that it may be advantageous in low-rise frames to count on the columns to carry the majority of the resistance to drift (say 40 to 45% to columns, and the rest divided about equally between the beams and connections). The use of fixed column bases is imperative in the design of PR-CC frames, just as it is in the design of almost all unbraced FR frames, in order to limit drifts. Thus, designers should pay careful attention to the detailing of the foundations and the column bases.

The required level of analysis for the design of unbraced frames with PR connections is currently not covered in any detail by design codes. The AISC LRFD specification [2] allows for the use of such connections by requiring that the designer provide a reliable amount of end restraint for the connections by means of tests, advanced analysis, or documented satisfactory performance. The AISC LRFD specification, however, does not provide any guidance on the analysis requirements except to note that the influence of PR connections on stability and P-Δ effects need to be incorporated into the design. The new NEHRP provisions and AISC seismic provisions [4, 28] will contain generic design requirements for frames with PR connections for use in intermediate and ordinary moment frames (IMF and OMF). In addition, it will contain some specific requirements for some specific types of connections, such as the PR-CCs described in this chapter. It is unlikely that there will be an attempt in the near future to codify the analysis and design of PR frames since it would be difficult to develop guidelines to cover the vast array of connection types available (Figure 23.1). Thus, design of PR frames will remain essentially the responsibility of the structural engineer with guidance, for particular types of connections, from design guidelines [8, 26], books [12, 13, 14], and other technical publications. The proposed procedures to be described next remain, therefore, only a suggestion for proportioning the entire system. Only the detailing of the connections, including checking all pertinent failure modes, should be regarded as a requirement.

The design procedure to be discussed is divided into two distinct parts. For the service limit states (deflections, drift, and vibrations) the design will use a linear elastic model with elastic rotational springs at the beam ends to simulate the influence of the PR connections. For the ultimate limit states (strength and stability), a modified, second-order plastic analysis approach will be used. In this case the connections will be modeled as elastic-perfectly plastic hinges and the stability effects will be modeled through a simplified second-order approach [26]. Because the latter was calibrated to a population of regular frames with PR-CCs, the approach is only usable for PR-CC frames. The design process will be illustrated with calculations for the frame shown in Figure 23.14. For a complete design example, including all intermediate steps and design aids, the reader is referred to [26].

EXAMPLE 23.4:

Conduct the preliminary design for the frame shown in Figure 23.14. The frame is a typical interior frame, has a tributary width of 30 ft, and will be designed for an 80 mph design wind and for forces consistent with UBC 1994 seismic zone 2A. The dead loads are 55 psf for the slab and framing and 30 psf for partitions, mechanical, and miscellaneous. The weight of the facade is estimated as 700 plf. The live loads are 50 psf and 125 psf in the exterior and interior bays, respectively, and will be reduced as per ASCE 7-95. The roof dead and live loads are 30 psf and 20 psf, respectively. The floor slab will consist of a 3-1/4 in. lightweight slab on a 3 in. metal deck, resulting is a typical Y2 for the slab of 4.5 in. The design of the entire frame is beyond the scope of this chapter, so calculations for only a few key steps will be given.

Part 1: Select beams and determine desired moments at the connections:

Step 1: Select the beam sizes based on the factored construction loads, as illustrated in Example 23.3. For this case the exterior bays require a W21x50, while the interior bays require a W21x44.

Step 2: Select moment capacity desired at the supports (M_{us}) based on the live loads. A good starting point is 75% of the M_p of the steel beam selected in Step 1, but the choice is left to the designer. Once M_{us} has been chosen, the factored moment at the center of the span (M_{uc}) can be computed as the difference between the ultimate simply supported factored moment (M_u, static moment) and M_{us}. For the interior span, $w_u = 6.66$ kip/ft and $M_u = 1020$ kip-ft of which roughly 55% corresponds to the dead loads and 45% to the live loads. Thus, select a connection capable of carrying:

$$M_{us} = 1020 \times .45 \times 0.75 = 330 \text{ kip-ft } = 3965 \text{ kip-in.}$$

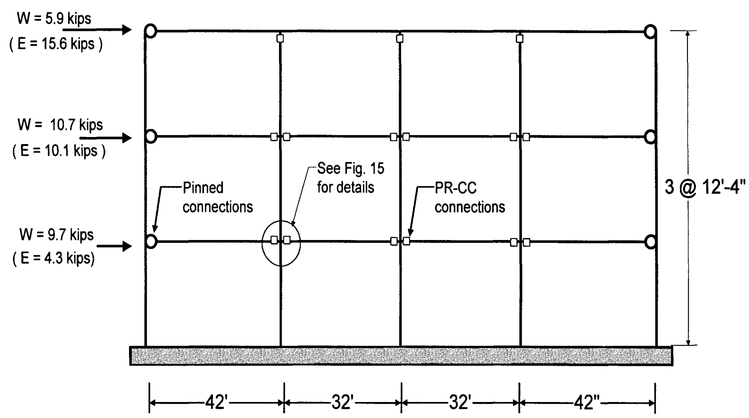

FIGURE 23.14: Frame for Example 23.4.

$$M_{uc} = 1020 - 330 = 690 \text{ kip-ft } = 8{,}280 \text{ kip-in.}$$

Step 3: Select a composite beam to carry M_{uc} and check that it can carry the unfactored service loads without yielding of the slab reinforcement. Assume that full composite action will be required to limit vertical deflections and lateral drifts. Using the steel beams from Step 1 and following the procedure from Example 23.3, the exterior bays require a W21x50 with 58 3/4 in. diameter studs, while the interior bays require a W21x44 with 52 studs. The design procedure for lateral loads was derived assuming that the beams were fully composite. In this case that means increasing the number of studs to 66 and 58, respectively, which is a very small increase. The moments of inertia computed from Equation 23.4, and including the contribution of the reinforcement are 1843 in.^{4} for the W21x44 and 1899 in.^{4} for the W21x50.

Part 2: Preliminary connection design:

Step 4: Compute the amount of slab reinforcement (A_{rb}) required to carry M_{us}. Assume that the moment arm is equal to the beam depth plus the deck rib height plus 0.5 in. The nominal required moment capacity is:

$$M_n = M_{us}/\phi = 3950/0.9 = 4388 \text{ kip-in.}$$
$$A_{rb} = 4388/\,(60 \text{ ksi } \times (21 + 3 + 0.5)) = 2.98 \text{ in.}^2$$

Try 8 #5 bars ($A_{rb} = 2.48$ in.^{2}). It is reasonable to use less area than required by the equations above ($A_{rb} = 2.98$ in.^{2}) because those calculation ignore the contribution of the web angles to the ultimate capacity and the $\phi = 0.9$ factor that has been added to the connection design. The latter accounts for the expected differences in stiffness and strength for the entire connection rather than for its individual components. Currently the LRFD Specification does not require such a factor and thus its use, while recommended, is left to the judgment of the designer.

Step 5: Choose a seat angle so that the area of the angle leg (A_{sL}) is capable of transmitting a tensile force equal to 1.33 times the force in the slab. The 1.33 factor is used to obtain a thicker angle so that its stiffness is increased.

$$A_{sL} = 2.48 * (60 \text{ ksi}/50 \text{ ksi}) * 1.33 = 3.95 \text{ in.}^2$$

Try a L7x4x1/2x8" ($A_{sL} = 4.00$ in.^{2}).

Step 6: For transferring the shear force consistent with the rebar reaching $1.25F_y$, the bolt shear capacity required is:

$$V_{\text{bolt}} = 2.48 \text{ in.}^2 \times 60 \text{ ksi } \times 1.25 = 186 \text{ kips}$$

This requires four 1-in. A490X bolts. Note that if the number of bolts is taken greater than 4, they would be difficult to fit into the commonly available angle shapes. In general the number and size of bolts required to carry the shear at the bottom of the connection is the governing parameter in design. Thus, another possible way of selecting the amount of moment desired at the connection (see Step 2) is to select the size and number of bolts and determine M_{us} as:

$$M_{us} = V_{\text{bolt}} \left(\text{beam depth } + \text{ deck height } + 0.5 \text{ in.} \right)$$

Step 7: Determine the number and size of bolts required for the connection to the column flange. From typical tension capacity calculations, including prying action, two 1-in. A490X bolts are required for the connection to the column. In general, and for ease of construction, these bolts should be the same size as those determined from Step 6.

Step 8: Select web angles (A_{wL}) assuming a bearing connection. Check bearing and block shear capacity. The factored shear (V_u) is:

$$V_u = 6.6(35/2) = 115.5 \text{ kips}$$

The factored shear from lateral loads is based on assuming the formation of a sidesway mechanism in which one end of the beam reaches its positive moment and the other its negative moment capacity. Since the connection has not been completely designed, assume that the negative and positive moment capacities are the same. This is conservative since the positive capacity will generally be smaller than the negative one.

$$V_u = 2M_{n,\text{conn}}/L = (4{,}388 \text{ kip-in. } + 4{,}388 \text{ kip-in.})/(35 \times 12) = 18.7 \text{ kips}$$

From Tables 9-2 in the LRFD Manual, four 3/4 in.-diameter A325N bolts, with a pair of L4x4x1/4x12" can carry 117 kips. Note that for calculation purposes, the area of the web angles (A_{Wl}) in Equations 23.1 and 23.2 is limited to the smallest of the gross shear area of the angles ($2 \times 12 \times 1/4 = 6.00$ in.^{2}) or 1.5 times the area of the seat angle ($1.5\ A_{Sl} = 1.5 \times 8 \times 1/2 = 6.00$ in.^{2}). This is required because Equations 23.1 and 23.2 were derived with this limit as an assumption.

Step 9: Determine connection strengths and stiffness for preliminary lateral load design. From Equations 23.3 through 23.5:

$$\begin{aligned}
k_{\text{conn}} &= 85\left[(4 * 2.48 * 60) + (6 * 50)\right](21 + 3.5) = 1.864 \times 10^6 \text{ kip-in./rad} \\
M_{u,\text{conn}} &= 0.245\left[(4 * 2.48 * 60) + (6 * 50)\right](21 + 3.5) = 5373 \text{ kip-in.} \\
k_{\text{ult}} &= 12\left[(4 * 2.48 * 60) + (6 * 50)\right](21 + 3.5) = 263.2 \times 10^3 \text{ kip-in./rad}
\end{aligned}$$

From the more complex Equation 23.1, the ultimate moment at 0.02 radians is 5040 kip-in., the secant stiffness to 0.002 radians is 1.403×10^6 kip-in./rad, and the ultimate secant stiffness is 252×10^3 kip-in./rad. Thus, the approximate formulas seem to provide a good preliminary estimate. Whenever possible, the use of Equations 23.1 and 23.2 is recommended.

The stiffness ratio for this connection is:

$$\alpha = 1.403 \times 10^6 \times (35 \times 12)/(29000 * 1699) = 11.95$$

Step 10: Check deflections under live load based on the service stiffness computed in Step 9. As for Example 23.3, the centerline deflection under full live loads is small since the α is large.

The connection designed in Steps 4 through 9 is shown in Figure 23.15. In the next steps, the adequacy of the connections, designed for gravity loads, to handle the design lateral loads will be checked.

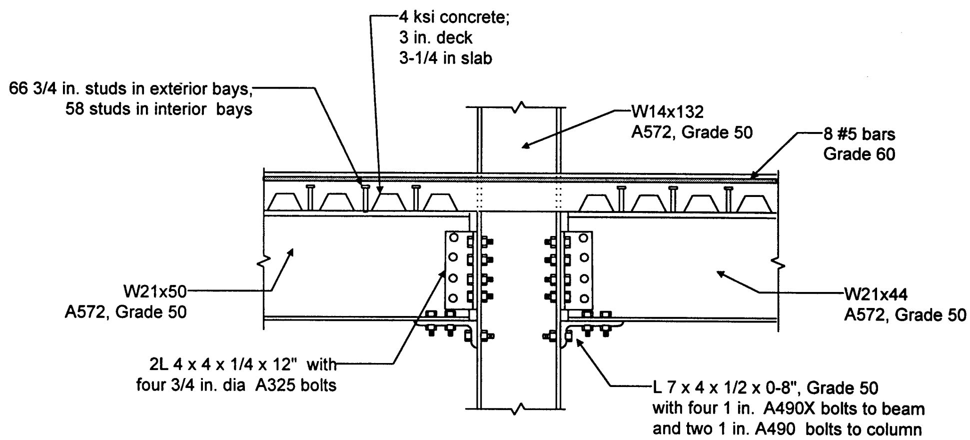

FIGURE 23.15: Connection details for Example 23.4.

Part 3: Preliminary lateral load design:

Step 11: Determine column sizes based on drift requirements and/or gravity load requirements. From the gravity loads, and making a 10% allowance for second order effects, a W14x74 was selected for the exterior leaner columns and a W14x132 for the interior columns. The selection of the interior columns was checked by satisfying the interaction equations (Equations H1-1a,b in the LRFD Specification) assuming that (a) the required moment capacity will be given by the summation of the moment capacities on either side of the connection ($M^-_{b,\text{conn}} = 4193$ kip-in. and $M^+_{p,\text{conn}} = 3655$ kip-in. from Equations 23.1 and 23.2); (b) the axial load is given by 1.2DL + 0.5LL ($P_u = 365$ kips, including live load reductions); and (c) B1 = 1.0 and B2 = 1.1.
The total story drift (Δ) can be calculated, for preliminary design purposes as:

$$\begin{aligned}
\Delta &= VH^2\left[\frac{1}{\sum K_c} + \frac{1}{\sum K_g} + \frac{1}{\sum K_{\text{conn}}}\right] \qquad (23.11)\\
\sum K_b &= \sum\left(\frac{12EI_{\text{eq}}}{L_b}\right) = \frac{(12)(29000)(2*1843+1898)}{(420)} = 4.635\times 10^6\\
\sum K_{\text{conn}} &= 4(1.403\times 10^6) = 5.612\times 10^6\\
\sum K_c &= \sum\left(\frac{12EI_c}{H}\right) = \frac{(2)(12)(29000)(1530)}{(148)} = 7.195\times 10^6
\end{aligned}$$

where

I_c and I_{eq} = the moments of inertia of the columns and beams

L_b = the girder length
H = the story height
V = the story shear
k_{conn} = the connection stiffness

For the girders the effective stiffness of the exterior girders, which are pin-connected at one end and have a PR connection at the other, was taken as equal to that of one girder. For the columns, only the two interior ones are used since the exterior ones are leaners. The summations are over all beams, columns, and connections participating in the lateral load resisting system. Note that for unbraced frames subjected to lateral loads one connection at each column line will be loading and one will be unloading. Thus, their k_{conn} should be different on either side of a column; however, for preliminary design it is sufficient to assume the k_{conn} for negative moments. For the critical first story, the shear (H) due to the wind loads is 26.3 kips. For drift design, this value will be checked against an allowable drift of 0.25%. From Equation 23.11, the interstory drift is 0.31 in. or $H/482$ which is well within the $H/400$ normally allowed. Note from the calculations of stiffness in Equation 23.11 that the connections actually provide about 32% of the lateral resistance. The beams provide about 27% and the columns provide the remaining 41%. This represents a well-balanced distribution of stiffness. Note again that the contribution of the columns, which is intimately tied to the assumption of base fixity, is the key to limiting drifts. The drift under seismic loads ($H = 34$ kips) can be checked roughly by calculating the elastic drift and multiplying it by an amplification factor (C_d). The new ASIC Seismic and NEHRP provisions give $C_d = 5.5$ for PR-CCs, and allow a maximum of 1.5% drift for this type of structure. Thus:

$$\Delta = (0.31 \text{ in.} \times (34/26.3) \times 5.5) = 2.20 \text{ in.} \rightarrow (2.20/148) \times 100 = 1.5\%, \text{ O.K.}$$

Although this frame barely meets the displacement criteria, a more refined non-linear analysis should be carried out to determine the actual drift.

Step 12: The strength of a frame can be calculated based on a sidesway, plastic collapse mechanism (Figure 23.16). The first-order, rigid-plastic collapse load factor (λ_p) for this type of structure is given by [26]:

$$\lambda_p = \frac{(N+1)M_{p,\text{col}} + ((N-1)*S)\left(M^+_{p,\text{conn}} + M^-_{p,\text{conn}}\right)_{\text{int}} + (S)\left(M^+_{p,\text{conn}} + M^-_{p,\text{conn}}\right)_{\text{ext}}}{\sum(V_i * H_i)} \tag{23.12}$$

where
N = the number of bays
S = the number of stories
V_i and H_i = the loads and heights at each story
$M_{p,\text{col}}$ = the column plastic capacity at the base
$M_{p,\text{conn}}$ = the connection capacity at 10 milliradians
ext and int refer to the exterior and interior connections
$+$ and $-$ refer to the positive and negative moment capacities.

For our case:

$$\lambda_p = \frac{(5)(10{,}530) + ((3)*2)(4193 + 3655)}{\sum(15.6*444 + 10.1*296 + 4.3*148)} = 9.45$$

This is apparently a very large collapse load factor, but there is a substantial reduction in that capacity due to second-order effects (Figure 23.17). Consideration of the P-Δ effects results in a second-order collapse load factor λ_k which is a function of the rigid plastic collapse load factor (λ_p) and the ratio (S_p) of the lateral displacement at collapse (Δ_k) to the displacement at a load factor of one (Δ_w). For proportional loading this leads to a second-order collapse load factor (λ_k) equal to [18]:

$$\lambda_k = \frac{\lambda_p}{1 + S_p \lambda_p^2 \left(\frac{\sum P\theta\delta}{\sum M_p \phi} \right)} \tag{23.13}$$

where

P = the axial loads
θ = the story rotation
δ = the elastic interstory drift
ϕ = the rotation of the plastic hinges
M_p = the moments at the hinges (Figure 23.16)

Values of S_p for various numbers of stories and story heights are given in Table 23.3. The ratio of θ/ϕ in the denominator of Equation 23.13 is equal to 1.0 when the member rotations (θ) are equal to the plastic hinge rotations (ϕ) as would be the case in the weak beam–strong column sway mechanism envisioned here. This results in $\lambda_k = 2.99$, which is a reasonable collapse load factor [17].

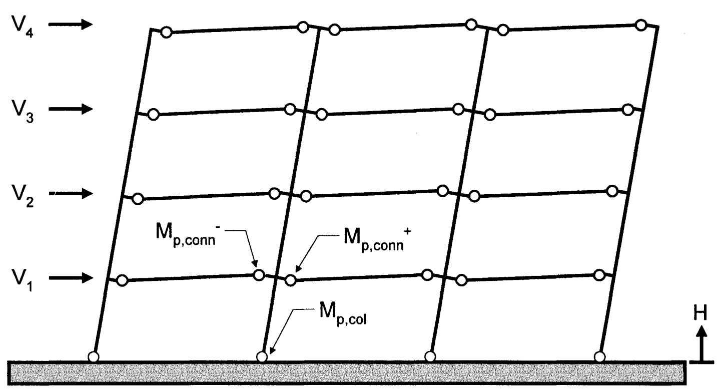

FIGURE 23.16: Plastic collapse mechanism and second order effects.

Step 13: Check strong column–weak beam behavior by requiring that:

$$1.25\left[\left(M^-\right)_{p,\text{conn}} + \left(M^+\right)_{p,\text{conn}}\right] \leq \sum \left(M_{p,\text{col}} \left[1 - \frac{P}{P_{\max}} \right] \right) \tag{23.14}$$

Step 14: Check stability of the columns by using AISC LRFD [2] Equation H1-1(a) and (b). Assume that lateral loads will control and that the maximum moments are equal to $M^+_{p,\text{conn}}$ plus $M^-_{p,\text{conn}}$. These $M_{p,\text{conn}}$ shall be based on a 1.25 overstrength factor for both rebar and steel angle, and a $\phi = 1.00$. For calculating G factors, assume that the effective moment of inertia for the beams is:

$$I_{\text{eff}} = I_{\text{eq}} \left(\frac{1}{1 + \frac{6}{\alpha}} \right) \tag{23.15}$$

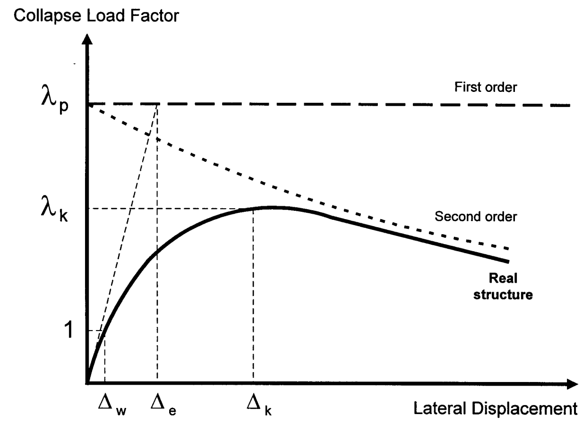

FIGURE 23.17: Simplified computation of plastic second-order effects. (After Horne, M.R. and Morris, L.J. *Plastic Design of Low-Rise Frames,* The MIT Press, Cambridge, MA, 1982.)

TABLE 23.3 Values of S_p

Number of stories	Story height (ft)	Proportional loading
	12	8
4	14	7.2
	16	5.4
	12	5.9
6	14	4.5
	16	3.9
	12	3.6
8	14	2.8
	16	2

From Hoffmann, J.J., Design Procedures and Analysis Tools for Semi-Rigid Composite Members and Frames, M.S. Thesis, University of Minnesota, Minneapolis. With permission.

Procedures for determining the stability of PR frames are still under development (see Chapter 3 of ASCE 1997 for more details).

Once a preliminary design has been completed, the final checks need to be made with advanced analysis tools unless the frame is very regular and seismic forces are not a concern. The level of modeling required is left to the discretion of the designer, but should, at a minimum, include tri-linear springs to model the connections and include second-order effects.

The design procedures illustrated here are limited to only one type of connection. To the author's knowledge only two other types of composite connections have received a similar level of development: those between steel beams and concrete columns and those for composite end plates. An extensive treatment of the general topic of connection design is given in Chapter 6 of Viest et al. [29]. The latest information on design of composite and PR connections can also be found in the proceedings of several international conferences [9, 10, 11, 19].

References

[1] ACI 318-95. 1995. Building Code Requirements for Reinforced Concrete (ACI 318-95), American Concrete Institute, Detroit, MI.

[2] AISC. 1993. *Load and Resistance Factor Design Specification for Structural Steel Buildings*, 2nd. ed., American Institute of Steel Construction, Chicago, IL.

[3] AISC. 1994. *Manual of Steel Construction—Load and Resistance Factor Design*, 2nd. ed., American Institute of Steel Construction, Chicago. IL.

[4] AISC. 1997. *Seismic Provisions for Structural Steel Building, Load and Resistance Factor Design*, American Institute of Steel Construction, Chicago, IL.

[5] Ammerman, D.J. and Leon, R.T. 1990. Unbraced Frames with Semi-Rigid Connections, *AISC Eng. J.*, 27(1), 12-21.

[6] Ang, K. M. and Morris, G. A. 1984. Analysis of Three-Dimensional Frames with Flexible Beam-Column Connections, *Can. J. Civ. Eng.*, 11, 245-254.

[7] ASCE. 1997. *Effective Length and Notional Load Approaches for assessing Frame Stability: Implications for American Steel Design*, 1st ed., ASCE, New York.

[8] ASCE Task Committee on Design Criteria for Composite Structures in Steel and Concrete. 1998, Design Guide for Partially-Restrained Composite Connections (PR-CC), *ASCE J. Struc. Eng.*, to appear in 1998.

[9] Bjorhovde, R., Colson, A., and Zandonini, R., Eds. 1996. *Connections in Steel Structures III: Behaviour, Strength and Design*, Proceedings of the Third International Workshop on Connections held at Trento, Italy, May, 1995, Pergamon Press, London.

[10] Bjorhovde, R., Colson, A., Haaijer, G., and Stark, J.W.B., Eds. 1992. *Connections in Steel Structures II: Behaviour, Strength and Design*, Proceedings of the Second Workshop on Connections held at Pittsburgh, April 1991, AISC, Chicago, IL.

[11] Bjorhovde, R., Brozzetti, J., and Colson, A., Eds. 1988. *Connections in Steel Structures: Behaviour, Strength and Design*, Proceedings of the Workshop on Connections held at the Ecole Normale Superiere, Cachan, France, May 1987, Elsevier Applied Science, London.

[12] Chen, W.F. and Toma, S. 1994. *Advanced Analysis of Steel Frames*, CRC Press, Boca Raton, FL.

[13] Chen, W.F. and Lui, E. 1991. *Stability Design of Steel Frames*, CRC Press, Boca Raton, FL.

[14] Chen, W.F., Goto, Y., and Liew, J. Y. R. 1995. *Stability Design of Semi-Rigid Frames*, John Wiley & Sons, New York.

[15] Eurocode 3. 1992. Design of Steel Structures, Part 1: General Rules and Rules for Buildings, ENV 1993-1-1:1992, Comite Europeen de Normalisation (CEN), Brussels.

[16] Goverdhan, A.V. 1984. A Collection of Experimental Moment Rotation Curves Evaluation of Predicting Equations for Semi-Rigid Connections, M.Sc. Thesis, Vanderbilt University, Nashville, TN.

[17] Hoffman, J. J. 1994. Design Procedures and Analysis Tools for Semi-Rigid Composite Members and Frames, M.S. Thesis, University of Minnesota, Minneapolis.

[18] Horne, M.R. and Morris, L.J. 1982. *Plastic Design of Low-Rise Frames*, The MIT Press, Cambridge, MA.

[19] IABSE. 1989. Bolted and Special Connections, Proceedings of the International Colloquium held in Moscow, USSR, May 1989, VNIPIP, 4 Vols., IABSE, Zurich.

[20] Kishi, N. and Chen, W. F. 1986. Data Base of Steel Beam-to-Column Connections, Vol. 1 & 2, Structural Engineering Report No. CE-STR-86-26, School of Civil Engineering, Purdue University, West Lafayette, IN.

[21] Leon, R.T. and Deierlein, G.G. 1996. Considerations for the Use of Quasi-Static Testing, *Earthquake Spectra*, 12(1), 87-110.

[22] Leon, R.T. 1996. Seismic Performance of Bolted and Riveted Connections, in *Background Reports on Metallurgy, Fracture Mechanics, Welding, Moment Connections and Frame System Behavior*, SAC Report 95-09, SAC Joint Venture, Sacramento, CA.

[23] Leon, R.T., Ammerman, D., Lin, J., and McCauley, R. 1987. Semi-Rigid Composite Steel Frames, *AISC Eng. J.*, 24(4), 147-156.

[24] Leon, R.T. and Hajjar, J.F. 1996. Effect of Floor Slabs on the Performance of Steel Moment Connections, Proceedings of the 11WCEE, Elsevier, London.
[25] Leon, R.T. and Zandonini, R. 1992. Composite Connections, in *Steel Design: An International Guide*, R. Bjorhovde and P. Dowling, Eds., Elsevier Publishers, London.
[26] Leon, R.T., Hoffman, J., and Staeger, T. 1996. Design of Partially-Restrained Composite Connections, AISC Design Guide 9, American Institute of Steel Construction, Chicago, IL.
[27] Nethercot, D.A. 1985. Steel Beam to Column Connections — A Review of Test Data and Their Applicability to the Evaluation of the Joint Behaviour of the Performance of Steel Frames, CIRIA, London.
[28] HEHRP. 1997. NEHRP Recommended Provisions for Seismic Regulations for New Buildings, BSSC, Washington, D.C.
[29] Viest, I.M., Colaco, J.P., Furlong, R.W., Griffis, L.G., Leon, R.T., and Wyllie, L.A. 1996. *Composite Construction Design for Buildings*, McGraw-Hill, New York.